

MESSENGER Mission: First Electronically Steered Antenna for Deep Space Communications^{1,2}

Robert S. Bokulic, Karl B. Fielhauer, Robert E. Wallis, Sheng Cheng,
M. Lee Edwards, Robert K. Stilwell, John E. Penn,
Jonathan R. Bruzzi, and Perry M. Malouf

The Johns Hopkins University
Applied Physics Laboratory
Laurel, MD 20723
240-228-6409
robert.bokulic@jhuapl.edu

Abstract— The MESSENGER mission to orbit the planet Mercury poses significant design challenges for its deep space communication system. These challenges include a wide pointing range, tight packaging, and a high temperature environment. To meet these challenges, the spacecraft incorporates the first steerable phased array antenna flown for deep space communications. The invention of a method for achieving circular polarization in a high-temperature (+300° C) environment has doubled the science return of the mission relative to its initially proposed implementation. Cross-strapping between the phased array antennas and solid state power amplifiers (SSPAs) enables both amplifiers to be turned on when sufficient power is available, enhancing the scientific return at the planet. A science return of 25 Gbits/year is achieved using only one SSPA in Mercury orbit. The science return increases to 100 Gbits/year if both SSPAs are used in the orbital phase.

TABLE OF CONTENTS

.....	
1. INTRODUCTION	1
2. RF COMMUNICATION SYSTEM DESIGN ...	2
3. PHASED ARRAY ANTENNA	3
4. SOLID STATE POWER AMPLIFIER.....	7
5. CONCLUSION.....	8
REFERENCES.....	8

1. INTRODUCTION

The MErcury Surface, Space ENvironment, GEOchemistry, and Ranging (MESSENGER) mission will launch from Cape Canaveral in May 2004 and begin a five-year journey to the planet Mercury. This mission will be the first to orbit that planet, spending one year gathering science data and transmitting it back to Earth [1]. Because of the inner planet trajectory and high temperature environment, the

mission presents challenging and unique problems to the radio frequency (RF) communication system.

Due to the geometry associated with an inner planet trajectory, the Earth can be in any direction about the spacecraft in a plane approximately aligned with the ecliptic. To provide such broad angular coverage for the science return, two X-band electronically steered phased array antennas, located on opposite sides of the spacecraft, are used. This approach, a first for deep space missions, is a departure from the traditional gimbaled dish antenna and was chosen because of the tight packaging requirements of the spacecraft and the high temperature environment near the Sun (+300° C).

The phased array subsystem, including antennas and redundant solid state power amplifiers (SSPAs), was developed at the Applied Physics Laboratory (APL) for the mission. Each phased array consists of a set of eight slotted waveguide “sticks” driven by a separate amplifier channel. Electronic steering in one dimension over a +/-45° range is accomplished by controlling the relative phases of the eight amplifier channels. Cross-strapping between the two redundant SSPAs and the phased array antennas provides block redundancy and, importantly, enables the RF power from both SSPAs to be applied simultaneously to either antenna. This feature gives the mission operators an option to increase the effective isotropic radiated power (EIRP) and downlink bit rate by a factor of four once in Mercury orbit.

This paper represents an update of an earlier paper [2], focusing on the significant design challenges that have been overcome and the resulting flight hardware performance. Following a review of the RF communication system design, the paper discusses the antenna and power amplifier technologies behind the design. The discussion includes the

¹ 0-7803-8155-6/04/\$17.00© 2004 IEEE

² IEEEAC paper #1370, January 16, 2004

invention of a new technique for producing circular polarization from a slotted waveguide stick in a high temperature environment. This invention enabled the science return of the mission to be doubled relative to the original (linearly polarized) design.

2. RF COMMUNICATION SYSTEM DESIGN

The primary requirement of the RF communication system is to return science data from the planet Mercury. This science return includes the data gathered from two flybys of the planet and an orbital phase lasting one year. Other important requirements of the system include command and telemetry capability over the entire mission, the return of science data from three Venus flybys, emergency mode communications, and real-time coverage of major engine burns. Shown below is a brief summary of the mission timeline (R_e = spacecraft-Earth distance; AU = astronomical unit):

- May 11, 2004: Launch from Cape Canaveral
- Nov. 2, 2004: Venus flyby #1 (R_e = 1.2 AU)
- Aug. 28, 2005: Venus flyby #2 (R_e = 1.2 AU)
- Oct. 22, 2006: Venus flyby #3 (R_e = 1.7 AU)
- Oct. 16, 2007: Mercury flyby #1 (R_e = 0.71 AU)
- July 7, 2008: Mercury flyby #2 (R_e = 0.96 AU)
- July 2, 2009: Mercury orbit insertion (R_e = 1.2 AU)
- July 2, 2010: End of mission (R_e = 1.3 AU)

The inner planet trajectory of this mission presents a challenging RF communications problem. This trajectory results in the need to provide a high gain downlink to Earth in all directions around the spacecraft. Thermal issues, tight spacecraft packaging requirements, and a strong desire to eliminate deployed components have precluded the use of a gimbaled reflector. As a result, an X-band phased array system has been adopted to enable high gain downlink communications.

The MESSENGER design incorporates two phased array antennas that are located diametrically opposite of each other and offset from the spacecraft-Sun line (Figure 1). Each array scans $\pm 45^\circ$ in one dimension. Through a combination of scanning and spacecraft rotation about the spacecraft-Sun line, the two arrays provide coverage over the entire sphere about the spacecraft³. The phased array beam is pointed by the spacecraft in an open-loop manner using on-board knowledge of the Earth direction. A key element in keeping the cost of this phased array system low was to make the design simple. This was achievable because the operational requirements could be met with a one-dimensional scanned phased array of passive radiating elements with transmit-only capability. The design uses an array of eight circularly-polarized slotted waveguides to withstand the thermal environment.

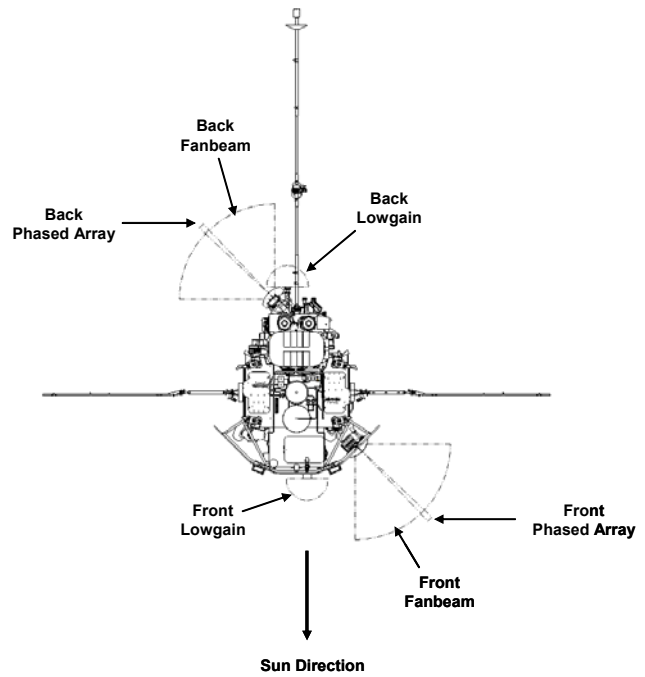
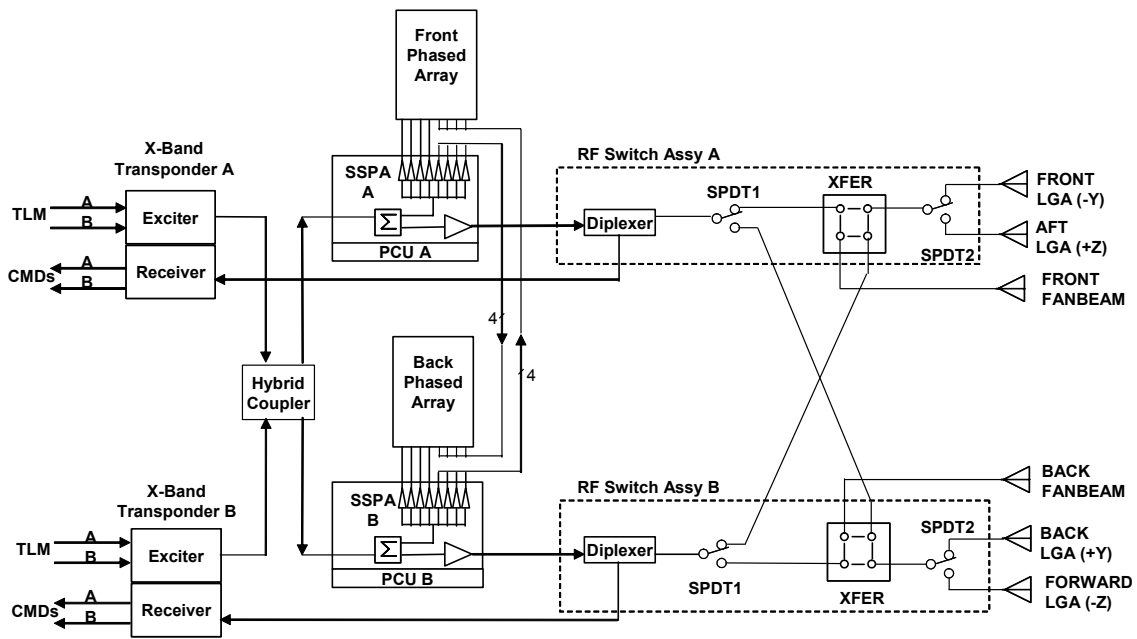


Figure 1. MESSENGER antenna pattern coverage (top view of spacecraft)

Figure 2 shows a block diagram of the RF communication system. Redundant X-band small deep space transponders, built by General Dynamics, are used to receive the uplink signal and generate the downlink signal. The downlink signal from each transponder is routed to the SSPAs using a passive hybrid coupler. Each SSPA consists of three separate amplifier sections, each with a total RF output power of at least 10 W. The “lumped” amplifier section provides the RF signal for the fanbeam and lowgain antennas. The first four outputs of the “distributed” amplifier section provide the RF signals for one phased array, while the second four outputs provide the RF signals for the other phased array. Only one of the three amplifier sections is powered at a time. Cross-strapping between the SSPAs and phased arrays ensures that no single failure can result in the loss of high gain antenna coverage on either side of the spacecraft. The minimum science return requirement of 16 Gbits in one year is exceeded with only one functional SSPA. Because of the cross-strapped design, enhanced scientific return is enabled when the spacecraft arrives at Mercury with two functional SSPAs. Enough solar array power is available to turn both SSPAs on, thereby increasing the effective radiated power (and science return) by a factor of four⁴. The expected science return is 25 Gbits/year using one SSPA and 100 Gbits/year using both SSPAs. Figure 3 shows the downlink bit rate profile using both SSPAs.

⁴The factor of four is achieved through a combination of doubled transmit power (from 11 to 22 W) and doubled aperture area (from 4 to 8 waveguide sticks).

³ The spacecraft is 3-axis stabilized.



All antennas are right-hand circular polarization.

Figure 2. Block diagram of the MESSENGER RF communication system

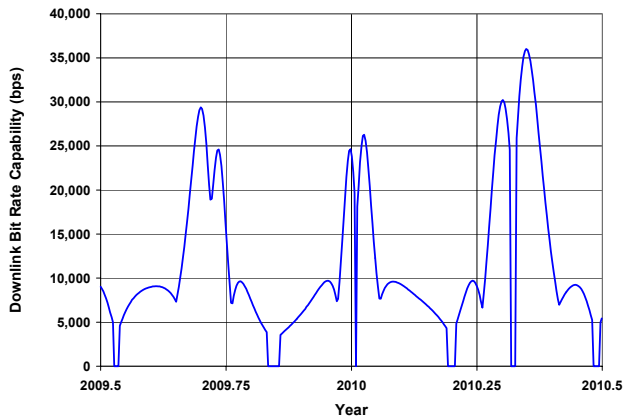


Figure 3. Downlink bit rate profile during the orbital phase using both SSPAs. The dips in the profile extending to zero are periods of solar conjunction.

3. PHASED ARRAY ANTENNA

Design Challenges

The design of the MESSENGER phased array antenna complies with several challenging requirements, such as the wide operating temperature range, one-dimensional electronic scanning, circular polarization and bandwidth. The wide operating temperature range is driven by the mission geometry. During the early portion of the mission, while the spacecraft is still relatively far from the Sun and heater power is limited, the antennas must operate at temperatures as low as -30°C and survive at temperatures as low as -100°C . In Mercury orbit, the Sun-facing front array is exposed to 11 times the solar radiation intensity as that observed at Earth, while the back array faces deep space. Even with the thermal protection of a radome, the predicted temperature of the front array at Mercury is as high as $+300^{\circ}\text{C}$. Except for the early months of the mission, the

back array temperature is controlled with a heater to approximately $+150^{\circ}\text{C}$. The high operating temperature of the front array limits the choices of radiating elements and circular polarization options to those that are comprised entirely of metal. The waveguide elements of both phased array antennas are identical in design.

Electronic scanning of each phased array in its broad plane minimizes the number of required phase shifter channels and minimizes the sensitivity of antenna gain to phase errors (the 3 dB beamwidth of the antenna pattern in the broad plane is a relatively wide 12.3°). An additional benefit of the phased array antenna for the downlink is its graceful degradation with failed amplifier modules. The effective isotropic radiated power (EIRP) is reduced by $20 \log(m/n)$, where m is the number of working modules and n is the total number of modules.

The challenge for circular polarization was driven by the desire to eliminate the 3 dB polarization mismatch loss between the inherent linear polarization of a slotted waveguide antenna element and the circular polarization of the Deep Space Network (DSN) ground stations. This challenge was magnified by the limited selection of antenna materials that could operate at $+300^{\circ}\text{C}$.

The bandwidth requirement of the array is driven primarily by the effects of thermal expansion of the antenna and to a lesser degree by the bandwidth of the transmitted signal. As the temperature of the array increases, the dimensions of the waveguide also increase and the effective center frequency of the antenna decreases. The bandwidth needed to account for this thermal expansion is given by:

$$BW_{\text{thermal expansion}} = 24\text{ppm}/^{\circ}\text{C} \times 400^{\circ}\text{C} = 0.96\%$$

where 24 ppm/°C is the thermal expansion coefficient of the aluminum waveguide and 400°C is the total temperature range. If we add 0.06% for the bandwidth of the downlink signal (5 MHz), then we get a total phased array bandwidth requirement of 1.02%. Because a slotted waveguide array is inherently narrowband, and the bandwidth reduces proportionally with the number of slots, this requirement limits the length of the phased array.

Design

The MESSENGER phased array is an array of eight waveguide “sticks,” each with 26 slotted radiating elements. Each waveguide stick is a standing wave array using narrow wall slots. A novel approach to achieve circular polarization was developed using sheet metal parasitic monopoles attached to the waveguide sticks [3]. The use of WR-90 aluminum waveguide with 0.051 cm (0.020”) thick walls keeps the mass of each waveguide stick less than 100 grams. The addition of a waveguide launcher, parasitic monopoles, and a titanium waveguide spacer brings the mass for each of the eight sticks to approximately 200 grams. The mass of the antenna assembly and its constituent parts, including the radome and fanbeam antenna, is given in Table 1. The design of the mounting plate represents a compromise between a low-mass design that requires extensive structural analyses and a conservative design that can be implemented on a short schedule. Figure 4 shows the phased array with eight radiating sticks, each 77.7 cm (30.6”) long, and two dummy⁵ waveguides that aid in achieving good circular polarization. With half-wavelength spacing between waveguide sticks, the width of the array, including the dummy waveguides, is 17.0 cm (6.7”). The waveguides are fed from the center. Although the standing wave array design is inherently narrowband, the center-fed approach results in a factor-of-two improvement in the impedance bandwidth compared with an end-fed approach and provides a measured 1 dB antenna gain bandwidth of 1.6%. Also shown in Figure 4 is the fanbeam antenna. Figure 5 shows some of the details of the phased array assembly from an end view.

The parasitic monopoles are attached to the waveguide using high temperature gold/germanium solder. The parasitic monopoles are etched from brass sheet stock and folded into final form. Both the aluminum waveguide and parasitic monopoles are gold-plated to allow attachment with the solder. A high quality solder joint is not only important for mechanical integrity but is also critical to the RF performance. The solder process, refined over the course of numerous temperature cycles and mechanical pull strength tests, provides a robust solder joint between the monopoles and the waveguide. The entire antenna assembly has been flight qualified through exposure to solar radiation intensity equivalent to that seen at Mercury (11

times that seen at Earth), thermal vacuum cycling between -100° C and +315° C, and vibration tests. The thermal testing was done at APL as well as the NASA Glenn Research Center. The vibration testing was done at APL.



Figure 4. Flight phased array assembly with radome removed. The fanbeam antenna is shown on the right side of the assembly.

The phased array radomes use space blanket materials that block light, withstand high temperatures, and have low dielectric constants and low dielectric losses. The radome is a three-layer design of 0.025 cm (0.01”) thick 3M™ Nextel™ blanket layers separated by 0.953 cm (0.375”) thick Q-felt material. Because the Nextel™ layers are thin and the Q-felt dielectric constant is low, the thickness of the Q-felt is not critical to RF performance. The chosen thickness is a compromise between low mass and light-blocking properties. The measured loss of the radome material is less than 0.1 dB over $\pm 45^\circ$ scan angles.

Coaxial-to-waveguide launchers are used at the inputs of the phased array to enable connection to the coaxial cables that drive it. A 4.8 cm (1.9”) long section of titanium waveguide is placed between the launcher and the input of each waveguide stick to provide thermal isolation. The inner dimensions of these titanium waveguides have been carefully chosen to enable the spacers to double as transmitter noise filters. The spacers each provide approximately 24 dB of reduction in the SSPA output noise floor at the uplink frequency (7.2 GHz). This filtering minimizes coupling of the SSPA noise into the spacecraft receiver through the fanbeam or lowgain antennas. The insertion loss of the spacer at 8.4 GHz is less than 0.1 dB.

⁵ The “dummy” waveguides are made of gold-plated aluminum but have no radiating slots.

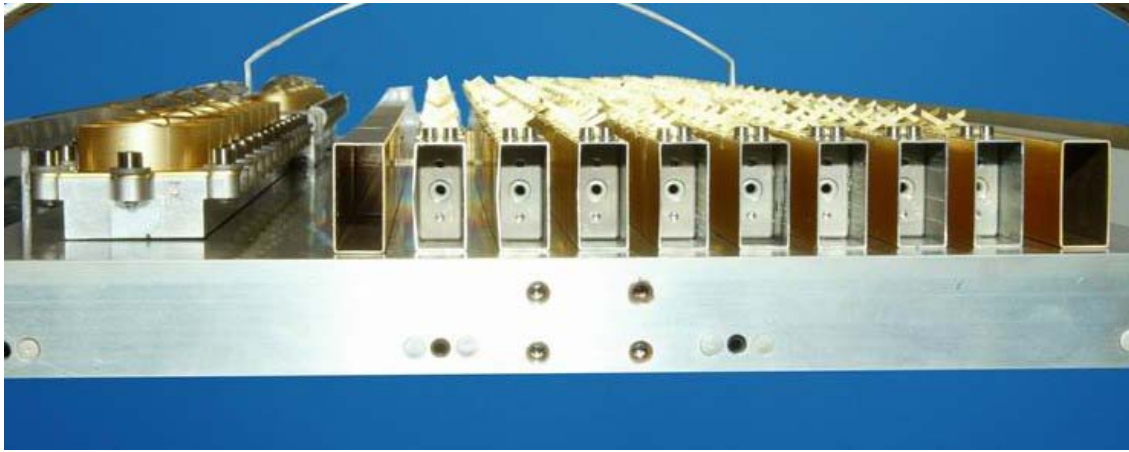


Figure 5. End view of the phased array assembly. The eight waveguide sticks of the phased array, with polarizers, and two “dummy” waveguides are visible. Adjustable short circuits, with tapped holes for the loop couplers, are shown at the ends of the waveguide sticks. The fanbeam antenna, with its helical radiating elements, is visible on the left side of the assembly.

Performance

Measurement of the performance of the phased array was a challenge because of the high temperature environment. Return loss measurements were made on the antennas over temperature to verify the center frequency and bandwidth of each individual stick. However, practical considerations limited our ability to measure radiation patterns over temperature. Instead, we varied the input frequency of the antenna to simulate the effect of temperature. The performance of the phased array antenna was measured using the APL indoor Compact Antenna Range. Return loss and element patterns were determined for each individual antenna stick in the arrayed configuration on the mounting plate. Return loss was better than 10 dB at 8.45 GHz and better than 7 dB across the expected effective frequency range (8.42 GHz to 8.49 GHz, corresponding to -43°C to $+303^{\circ}\text{C}$). The relative radiated phases of the sticks were also measured for use in determining the optimal steering lookup table in the final spacecraft configuration.

A commercial set of phase shifters was used to electrically steer the phased array to determine its full radiation pattern. This technique enabled us to test the antenna without the SSPAs⁶. A scheme was developed to expedite the process of measuring the antenna gain at every degree of electrical scan by interfacing the Compact Antenna Range software with the phase-shifter control software. Antenna gain was measured at each degree of electrical scan between -60° and $+60^{\circ}$ from the broadside direction as the antenna was mechanically scanned through the transmit path. This procedure allowed electrically scanned “gain envelopes” to be determined relatively quickly.

Radiation patterns for each flight phased array included gain envelopes of the 8-stick full array and the two 4-stick half arrays. The narrowbeam pattern in the broadside direction was also measured, as well as the broadbeam pattern at every 15° of electrical scan between -45° and $+45^{\circ}$ from the broadside direction. All patterns included data across a frequency range that encompassed the operating temperature range of the antenna (-30° to $+300^{\circ}\text{C}$). Figure 6 shows the measured envelope gain pattern as a function of scan angle for various operating temperatures (simulated by varying the center frequency). Table 1 summarizes the measured performance parameters of the phased array antenna at $+300^{\circ}\text{C}$.

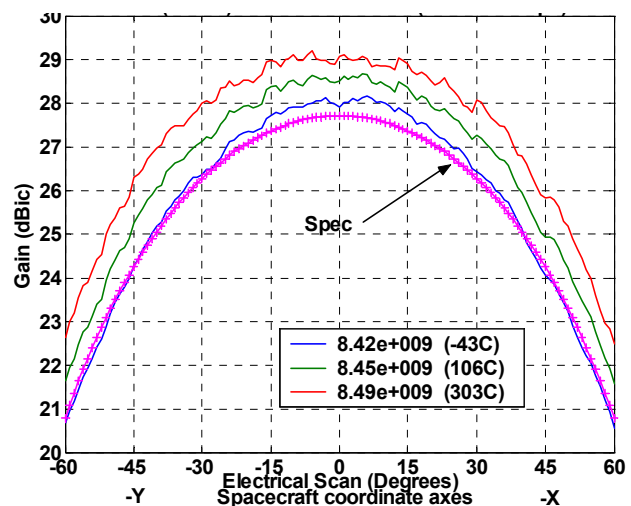


Figure 6. Typical phased array gain envelope pattern. This plot shows the peak gain as a function of electrical scan angle and array temperature.

⁶ Both phased arrays were also tested as a system with the SSPAs.

System-Level Testability

To minimize the radiation hazard to personnel, all antennas are fitted with an absorptive “hat” cover for use during spacecraft-level testing. However, this cover and other practical issues prevent measurements of the radiated antenna pattern at the spacecraft level. To enable such measurements, a novel loop coupler⁷ has been developed to sample the signal at each waveguide stick. A coupler is installed through a small hole in the short circuit at the end of each waveguide stick for ground testing and is removed prior to launch. The magnitude and phase of the coupled signal is referenced to the magnitude and phase of the waveguide launcher input and radiated signals. The radiated array pattern can then be calculated using measurements from the eight couplers and knowledge of the individual stick element patterns. The calculated pattern using the loop couplers shows excellent agreement with the ideal sum of the eight stick element patterns as shown in Figure 7.

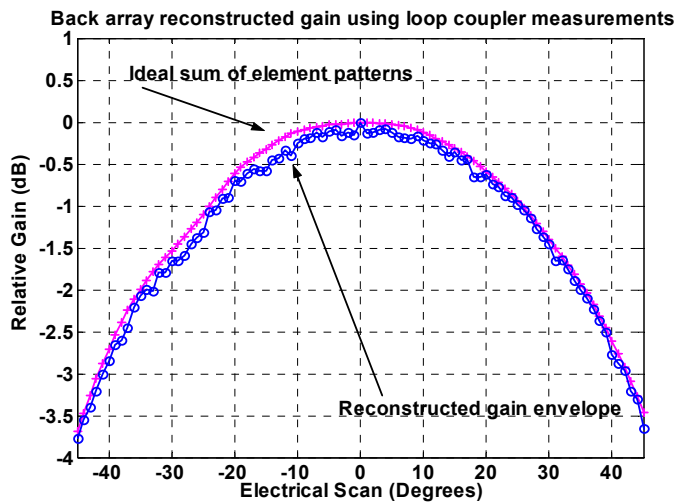


Figure 7. Comparison of envelope pattern calculated from loop coupler measurements and the ideal element pattern sum.

Fanbeam Antenna

The fanbeam antenna is used for reception of the uplink signal at 7.2 GHz over the entire mission and simultaneous transmission of the downlink signal at 8.4 GHz during special periods of the mission such as emergency mode. The gain of its wide-plane pattern varies between about +12 and +16.5 dBic⁸ over a range of $\pm 45^\circ$ from broadside. The 3 dB beamwidth of the narrow-plane pattern is about 7° . The axial ratio along the wide-plane pattern is generally less than 4 dB at both frequencies of operation.

⁷ A small loop connected to an SMA connector samples the intensity of the local magnetic field.

⁸ The unit “dBic” denotes gain relative to an isotropic circularly-polarized radiator.

The fanbeam antenna is a WR-112 waveguide-based design comprised of a diplexer, an uplink array, and a downlink array. Both arrays are standing wave antennas consisting of a length of waveguide that is shorted at one end. The radiating elements are short helices centered on the broad wall of the waveguide and located at the maxima of the standing wave in the waveguide (half guide-wavelength spacing). Each helix has a probe that extends into the waveguide and is excited by a maximum in the standing wave pattern. The reactive portion of the helix probe admittance is tuned out by a thin shunt inductive iris in the waveguide, with one iris at each probe location. The helices provide the required right-hand circularly polarized radiation. Figure 8 shows a close-up view of the helical elements.

Metal waveguide construction enables the antenna to survive the extreme temperature range of the mission environment (-100°C to $+300^\circ\text{C}$). The helix probes are incorporated into a feedthrough consisting of a glass-to-metal seal. Each helix assembly is then soldered into the broad wall of the waveguide.

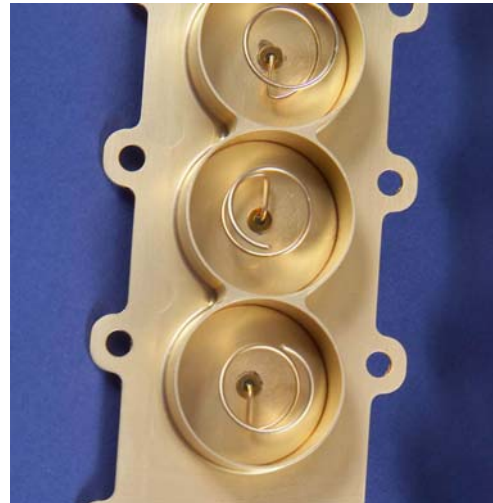


Figure 8. Detailed photo showing helical antenna elements of the fanbeam antenna.

Table 1
Typical Phased Array System Performance
(Measured flight hardware performance)

Phased Array Antenna (Performance of 8-stick array at typical operating temperature of +300° C)		
Broadside gain	29.0 dBic	
Scanning loss	Loss= $\cos^n(\theta)$ where $n=2.4$ θ is the scan angle from broadside direction	
Axial ratio	≤ 2 dB at broadside ≤ 3 dB over $\pm 45^\circ$ scan	
Polarization	Right-hand circular (RHC)	
3 dB beamwidth	12.3° (broad plane) 2.5° (narrow plane)	
Return loss	15 dB	
1 dB gain bandwidth	135 MHz (1.6% of center frequency)	
Mass	1.68 kg (phased array waveguide elements) 1.38 kg (radome) 0.69 kg (fanbeam antenna and diplexer) 3.12 kg (mounting plate and hardware)	
SSPA (Performance at typical operating temperature of +20° C)		
	Distributed Amplifier	Lumped Amplifier
RF output power	11 W average over all phase states (2.75 W per output)	10 W
DC power at 28 V	40 W (SSPA) 8 W (PCU) 48 W (total)	39 W (SSPA) 7 W (PCU) 46 W (total)
Output RF power compression	2 to 4 dB	3 to 4 dB
Input return loss	≥ 12 dB	
Output return loss	≥ 20 dB	≥ 20 dB
AM/PM conversion	≤ 3 °/dB	≤ 4 °/dB
RF input power (to produce rated output power)	+6 dBm	+6 dBm
Harmonics	≤ -30 dBc	≤ -30 dBc
Phase shifter resolution	22.5°	N/A
Phase shifter accuracy	4.3° rms	N/A
Mass	1.2 kg (SSPA) 0.61 kg (PCU)	
System-Level (includes phased array antennas, SSPAs, and interconnecting cables)		
Passive loss between SSPA and phased array antenna	1.7 dB average loss for eight-stick phased array	
Phase error among waveguide sticks within each phased array	4.7° rms, random 16.2° peak, systematic	
Gain reduction due to systematic and random phase errors among waveguide sticks	0.07 dB typical 0.41 dB worst case	

4. SOLID STATE POWER AMPLIFIER

The detailed design and essential technologies of the X-band SSPA were presented in an earlier paper [2]. Here we present an overview of the design and technologies, then discuss the significant changes since the earlier paper and, finally, present the flight hardware performance results.

Design Overview

The SSPA is comprised of three microwave amplifier sections and two multilayer printed circuit boards in a common aluminum chassis. It contains a “lumped” amplifier section that outputs an RF signal for the fanbeam and lowgain antennas on the spacecraft. It also contains two “distributed” amplifier sections with four amplifiers in each section. Each of these two sections (distributed 1-4 and distributed 5-8) is powered separately and provides output signals for the two phased array antennas. Only one amplifier section is powered at a time by controlling the application of secondary power supply voltages using mechanical relays in the SSPA.

An RF power divider board contains the mechanical relays and an 8-way RF power divider used to drive the distributed amplifiers. A digital board contains a MIL-STD-1553 bus interface hybrid, an ACTEL field-programmable gate array, and a telemetry interface chip. This board is used to control the 4-bit phase shifter in each channel of the distributed amplifier sections and to send housekeeping telemetry back to the spacecraft command and data handling system.

Conditioned power is supplied to the SSPA by an external power converter unit (PCU) purchased from EMS Technologies. The PCU supplies the necessary -5, +5, +6.5/7.0, and -15 volt DC power and provides the power-on and power-off sequencing of the voltages needed to prevent damage to the SSPA.⁹

The RF input power to the SSPA is held relatively constant at a level of +6 dBm by controlling the temperature of the transponders that drive it on the spacecraft. Tailoring of the SSPA consists of using temperature-compensated chip attenuators within the unit to produce the required RF output power and compression levels over temperature. The RF output power levels of the lumped section and each distributed section are 10 W and 11W, respectively.

Microwave Technologies

The power amplifier lineups used in the SSPA incorporate established GaAs-based MESFET, HFET, and pHEMT devices from Triquint Semiconductor in Dallas, Texas. A photograph of the SSPA assembly is shown in Figure 9.

The RF output signal of the lumped amplifier is generated by the parallel combination of four Triquint 9083 power amplifier chips. Fusing is used to prevent a short circuit in

⁹ The distributed amplifier channels require 6.5 volts for their drain terminals, while the lumped amplifier requires 7.0 volts for its drain terminals. A configuration indicator fed from the SSPA to the PCU controls the voltage level.

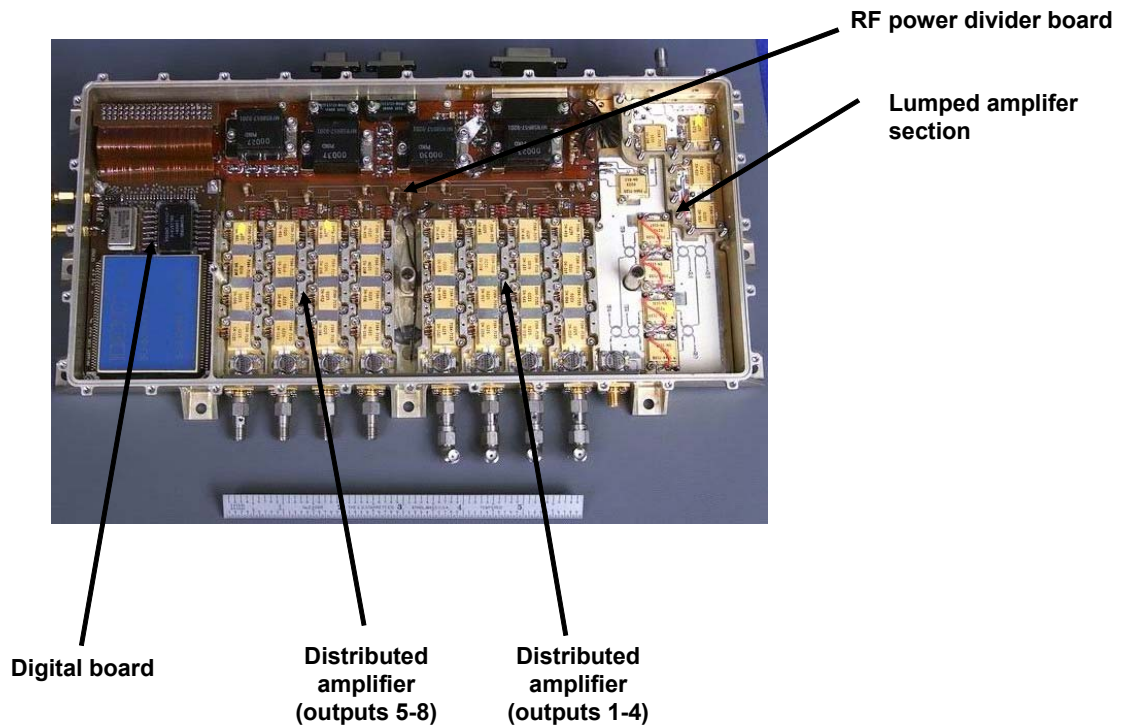


Figure 9. Photograph of the solid state power amplifier

one of the chips from taking down the entire amplifier section, thereby protecting the inherent redundancy in the parallel amplifier arrangement. The RF output signals from the distributed amplifiers are each generated by a single Triquint 9083 power amplifier chip. Fusing is again used to prevent a short circuit in one of the channels from taking down the remaining three channels, thereby protecting the inherent redundancy in the phased array. Driver amplifiers in the SSPA incorporate either the Triquint 8810 amplifier chip or the Triquint 4230 and 4240 HFET transistors with appropriate matching circuits. The 4-bit phase shifter in each distributed amplifier channel is a Triquint 6336 device. All of the GaAs devices used in the SSPA are housed in individual APL-designed hermetic packages made by Kyocera. The chip devices were packaged and screened to MIL-PRF-38534 hybrid microcircuit specifications at APL [4].

Performance

The measured performance of the SSPA at +20° C is given in Table 1. These values are representative of the performance of the unit over its specified temperature range of -10° to +40° C.

5. CONCLUSION

This paper has presented the technologies and performance of the first steerable phased array to be used for a deep space communication system. The complexity and cost normally associated with phased arrays has been minimized by simplifying the requirements including the incorporation of passive radiating elements, one-dimensional scanning, and transmit-only operation. The phased array approach

was adopted because the high temperature environment at Mercury and the tight packaging requirements of the spacecraft precluded the use of a gimbaled dish antenna.

Key technology developments include a novel method for achieving circular polarization from slotted waveguides, the use of high temperature techniques and materials, and a densely packaged X-band solid state power amplifier. Subsystem-level innovations include the use of cross-strapping to enable a potential factor-of-four increase in scientific return and a simple method of monitoring the beam steering performance of the phased array at the spacecraft level without radiating.

While the MESSENGER mission has unique requirements, particularly high-temperature antenna operation, the technologies and techniques developed for this mission should be useful for a wide range of civilian and military aerospace applications.

REFERENCES

[1] A. G. Santo et al., "The MESSENGER Mission to Mercury: Spacecraft and Mission Design," *Planetary and Space Science*, Vol. 49, pp. 1481-1500, 2001.

[2] R. E. Wallis and S. Cheng, "Phased-Array Antenna System for the MESSENGER Deep Space Mission," *IEEE Aerospace Conference Technical Digest*, March 2001.

[3] R. K. Stilwell, R. E. Wallis, and M. L. Edwards, "A Circularly Polarized, Electrically Scanned Slotted Waveguide Array Suitable for High Temperature Environments," *IEEE Antennas and Propagation Society International Symposium Proceedings*, Vol. 3, pp. 1030 - 1033, June 22-27, 2003.

[4] E. Nhan et al., "Recent Test Results of a Flight X-Band Solid-State Power Amplifier Utilizing GaAs MESFET, HFET, and pHEMT Technologies," *2002 GaAs Reliability Workshop Proceedings*, pp. 37-44, Oct 20, 2003.

ACKNOWLEDGEMENT

The MESSENGER project is sponsored by the NASA Office of Space Science as part of its Discovery Program.

BIOGRAPHIES



Robert S. Bokulic is a member of the Principal Professional Staff and assistant supervisor of the RF Engineering Group at APL. He served as the lead engineer responsible for the MESSENGER RF communication system during the development and implementation phases of the program. Mr. Bokulic received a B.S. degree in electrical engineering from Virginia Tech in 1982 and an M.S. degree in electrical engineering from The Johns Hopkins University in 1985. He joined the APL Space Department in 1982 and has specialized in spacecraft communication systems since then. Mr. Bokulic's interests include a combination of communication systems engineering and associated technology development. He is a member of the IEEE.



Karl B. Fielhauer is currently the lead engineer responsible for the MESSENGER RF communication system. He is also the supervisor of the RF Systems Engineering Section of the RF Engineering Group at APL. He received a B.S. in 1985 from Lawrence Technological University in Southfield, Michigan, and a M.S.E.E. in 2002 from The Johns Hopkins University in Baltimore, Maryland. Before joining APL, Mr. Fielhauer worked for the Department of Defense and Litton's Amecom Division in College Park, Maryland. Since joining the APL Space Department in 1997, he has focused primarily on the design and development of digital hardware for the TIMED and CONTOUR missions and their ground support equipment. Mr. Fielhauer was previously the Lead RF Communications Engineer on the CONTOUR mission and is a member of IEEE.



Robert E. Wallis is currently the Lead Engineer for the MESSENGER Phased-Array System. He received his B.S. from the Pennsylvania State University in 1980 and his M.S. from Villanova University in 1983, both in electrical engineering. He joined the APL Space Department in 1999 and is currently supervisor of the Microwave Systems Section of the RF Engineering Group at APL. From 1983 to 1999, Mr. Wallis was with EMS Technologies, Inc. (formerly Electromagnetic Sciences Inc.), where he managed the Microwave Integrated Circuit (MIC) design group and led the development of switch matrices and SSPAs for spacecraft applications, including C-band SSPAs for the TOPEX mission, X-band SSPAs for the Mars98 and Stardust missions, and Ku-band SSPAs for the International Space Station. From 1980 to 1983, Mr. Wallis was with General Electric Space Systems Division in Valley Forge, Pennsylvania, as a member of the MIC design group.



Sheng Cheng is currently the Lead Engineer for the MESSENGER Solid-State Power Amplifier. He received his B.S. from the National Taiwan University in 1982 and his M.S. from The Johns Hopkins University in 1989, both in electrical engineering. He joined the APL Space Department in 1997 as a senior microwave circuit design engineer in the RF Engineering Group. From 1990 to 1997, Mr. Cheng worked at the Whiting School of Engineering of The Johns Hopkins University on the research and development of microwave circuit theory, design methodology and measurement techniques. Prior to that, Mr. Cheng was with the LKC Technologies in Gaithersburg, Maryland, as an electronic circuit design engineer.



M. Lee Edwards, Ph.D., received the B.S. and M.S. degrees in electrical engineering from N.C. State University and Northwestern University, respectively, and the Ph.D. degree in mathematics from the University of Maryland. He is supervisor of the RF Engineering Group in the Space Department of the Applied Physics Laboratory and chairs the Electrical and Computer Engineering Program in the JHU School of Engineering. He has been a leader in both the R&D and educational aspects of microwave engineering. His experience includes the design and analysis of microwave integrated circuits (MICs) and monolithic microwave integrated circuits (MMICs). He is a senior member of the IEEE and a member of Eta Kappa Nu, Tau Beta Pi, Pi Mu Epsilon, Phi Kappa Phi, and sigma Xi.



Robert K. Stilwell is a member of the Senior Professional Staff, specializing in antenna design and analysis, in the RF Engineering Group of the APL Space Department. He developed the method of achieving circular polarization used by the MESSENGER phased array. Mr. Stilwell received his B.S. from Kansas State University in 1973 and his M.S. in 1976 from The Johns Hopkins University, both in electrical engineering. He joined the APL Space Department in 1973 and has since been primarily engaged in the design and development of antenna systems. These have ranged from broadbeam wire antennas operating at VHF to high gain reflector antennas for radar altimetry. Mr. Stilwell has contributed to systems that have flown on over twenty spacecraft.



John E. Penn received a B.E.E. from the Georgia Institute of Technology in 1980 and M.S. degrees in Electrical Engineering and Computer Science from The Johns Hopkins University in 1982 and 1988. His work has involved custom integrated circuit design, digital design, microwave design, and monolithic microwave integrated circuit (MMIC) design.

Mr. Penn is employed in the Space Department of the Applied Physics Laboratory as a member of the RF Engineering Group and co-teaches a MMIC design course with Mr. Craig Moore at The Johns Hopkins University (EE787).



Jonathan R. Bruzzi is a member of the Associate Professional Staff in the RF Engineering Group at APL. He is the lead engineer for the MESSENGER low gain antennas and was also responsible for the phased array control, calibration, and measurement test processes. He received his B.S.E. in electrical engineering in 1999 and his M.S.E.

in electrical engineering in 2000, both from the University of Pennsylvania. He joined the APL Space Department in 2000 specializing in antennas, electromagnetics, and optical communications.



Perry M. Malouf, Ph.D., is a member of the Senior Professional Staff in the RF Engineering Group of the APL Space Department. He received his B.S., M.S., and Professional Engineer degrees from Columbia University in New York, NY in 1982, 1983, and 1985, respectively, all in electrical engineering. He received his Ph. D. in electrical engineering from the University of Maryland, College Park in 1994. Dr. Malouf joined APL's Space Department in 1997 and began working on X-band high efficiency solid state power amplifiers. He then moved on to waveguide antenna design and was the lead engineer for the MESSENGER medium gain (fanbeam) antenna. From 1995 to 1997, Dr. Malouf was with Stanford Telecom in Annapolis Junction, MD. From 1985 until 1994 he was at the U. S. Naval Research Laboratory, where he performed research in the area of gyrotrons (1988 to 1994) and also performed antenna analysis (1985 to 1988). Dr. Malouf specializes in electromagnetics and is a member of the IEEE and the APS.